Positionally-independent and extended read range resonant sensors applied to deep soil moisture monitoring

By Yee Jher Chan[†][a], Adam R. Carr[†][a], Subhanwit Roy[b], Caden M. Washburn[a], Nathan Neihart[b] and Nigel F. Reuel*[a]

† Authors contributed equally to this project.

[a]Department of Chemical and Biological Engineering, Iowa State University, Ames, IA 50011

[b]Department of Electrical and Computer Engineering, Iowa State University, Ames, IA 50011

*Corresponding author reuel@iastate.edu

ABSTRACT

Here we detail an inductively coupled extender (ICE) and resonant (LC) sensor to monitor soil moisture using a portable reader. Significant advances of this ICE-LC design are extending typical LC sensor read range over a meter and reducing positional alignment sensitivity between reader and sensor. An analytical model validates the working principle and feasibility of the ICE-LC system. Prototypes of the ICE-LC sensor were built and optimized in terms of sensitivity and power transfer (single and four turns for ICE top and bottom coils, respectively). Soil moisture tests validated the ICE-LC improvements on minimized positional alignment sensitivity and extended read range, transducing a decrease in resonant frequency with increasing soil moisture. When calibrating with existing wired approaches, the ICE-LC sensor had a reproducible, linear sensor gain of 4.52 %moisture content/MHz with an R^2 of 0.745 and RMSE of 2.41%. A smaller, planar form factor of the ICE-LC sensor was also tested and

exhibited reduced positional alignment sensitivity between reader and sensor at shorter read ranges. This initial study demonstrates the feasibility of the ICE-LC resonant sensor as a cost-effective method to monitor soil moisture content throughout the growing season at many field locations.

KEYWORDS

Inductive-capacitive sensor, precision agriculture, soil moisture sensing, embedded sensor, radio frequency

INTRODUCTION

Soil moisture content is a critical environmental parameter which is significant to many scientific and commercial fields. It determines the soil's structure, moderates its temperature, serves as a transport medium for chemicals, and provides the means for life to grow(Topp, Parkin and Ferre, 2006). Soil moisture content is a key parameter in weather and climate models, closing the energy and mass balances due to evapotranspiration processes between land and atmosphere(Dirmeyer *et al.*, 2016). Geotechnical engineering uses soil moisture content during shrink-swell and strength tests of cohesive soils to ensure the soil has proper mechanical properties before constructing infrastructure on it(Das and Sivakugan, 2015). Measuring soil moisture content is also extremely important to agriculture and crop management. In particular, it determines the field capacity of soil which is the water retained in soil after being saturated and allowed to freely drain. Known field capacity is critical to monitor

to avoid the permanent wilting point of a crop, where the moisture content drops below a point where the plant is capable of recovering(Cassel and Nielsen, 1986).

Continuous monitoring of soil moisture content, rather than sporadic measurements, is necessary to update climate models and improve crop management practices. It is also advantageous to obtain measurements at multiple depths. Field capacity changes with root depth relative to the water table which also varies throughout the growing season. Continuous soil moisture monitoring can help prevent crop failure. It can inform real-time dosing of additional irrigation volume, avoiding situations of under and over watering, thereby improving the economics and sustainability of field management practices.

Current methods to monitor soil moisture content include remote and *in situ* methods. Remote methods include microwave remote sensors(Sure and Dikshit, 2019; Franceschelli *et al.*, 2020), cosmic ray neutron probes(Franz *et al.*, 2016), ground penetrating radar(Steelman and Endres, 2011), electromagnetic induction(Martini *et al.*, 2017), optical(Babaeian *et al.*, 2019), thermal remote sensors(Crow, Kustas and Prueger, 2008). These remote sensors are contactless and do not require being buried in the soil although in most cases they can only measure soil moisture content at or near-surface level with sensing depth of ~5-10 cm(Calvet *et al.*, 2011). They are especially useful in meteorological applications and climate models as the near-surface region is the most dynamic region in terms of soil moisture content. Hydrological models can be implemented to extrapolate the soil moisture content to the root zone (>1m depth) from near-surface measurements(Mohanty *et al.*, 2017), however truth data from *in situ* sensors need to be deployed to validate the accuracy of such models. There are several *in situ* sensors which are implemented, including time domain reflectometry(Topp, Davis and Annan, 1980), frequency

domain reflectometry(Xu *et al.*, 2014), capacitive(Goswami, Montazer and Sarma, 2019), and resistive(Saleh *et al.*, 2016). All of these are electromagnetic based sensors, the first three of which measure the relative permittivity of the soil which changes with soil moisture content (relative permittivity of water and bulk soil is approximately 80 and 3 respectively). Resistive sensors tend to be more susceptible to electrolytic corrosion and soil ion concentration and are therefore not used in long term deployments(Nagahage, Nagahage and Fujino, 2019). These and other *in situ* sensors have provided truth data which feed into and validate climate and hydrological models, especially through the widespread work of the International Soil Moisture Network(Dorigo *et al.*, 2011) and North American Soil Moisture Database(Quiring *et al.*, 2016). There are limitations of the currently implemented *in situ* sensors. All of these previously discussed sensors are active and require a connection to a permanent power supply. The individual price point per sensor and need for centralized data acquisition and power hubs limit the number of measurement nodes that can be deployed; these are typically focused on few measurement sites and do not allow for monitoring heterogenous soil moisture content throughout the field.

LC resonant sensors provide an alternative approach for monitoring soil moisture content. LC resonators include an inductor and capacitor (either discrete or parasitic) which resonate at a specific frequency(Huang, Dong and Wang, 2016). This frequency is influenced by changes in the relative permittivity of their surrounding environment giving them the same working principle as other currently used soil moisture sensors; LC sensors have been used to monitor aqueous samples with volumetric moisture changes(Carr *et al.*, 2020; Charkhabi *et al.*, 2020; Mohammadi *et al.*, 2020). Key benefits of resonant sensors are their ultra-low cost point

enabled by facile fabrication methods (screen printing with no pick and place of integrated circuits(Charkhabi *et al.*, 2020)) and no on-board battery or wireless power transfer circuitry (e.g., rectifier and capacitor);this allows them to be deployed in many locations, providing holistic measurement of a heterogenous environment. They can be wirelessly and passively activated through non-metallic materials by the interrogation reader, i.e. they do not require a tethered power supply or data connection to read moisture content under the soil., There are two issues of current LC resonant sensors that limit their widespread use in many applications. First, their read range is limited to a short distance (<5 cm), and second, their signal is sensitive to misalignments between the wireless reader and the LC-resonator; to date this has required stationary and close reader placement during measurement to help mitigate these limitations.

Attempts have been made to overcome these limitations. The read range can be increased through the use of repeater frequency coils(Zhang, Wang and Huang, 2014; Dong *et al.*, 2016), increased quality factors(Nopper, Niekrawietz and Reindl, 2010), and increased inductive element size(Park *et al.*, 2004). These can improve read range through free medium like air but are not as effective in lossy systems like wet soil. Sensitivity to misalignment can be overcome through the use of novel reader architectures(Nopper, Has and Reindl, 2011; Babu and George, 2018) and interpolating the position of reader/sensor alignment with an array of LC resonators(Chan *et al.*, 2020). To this point, however, no attempt has been made to both increase the read range and mitigate misalignment issues in the same reader/sensor architecture.

This study presents a novel LC-resonant sensor architecture which both increases read range and lessens the effects of reader/sensor misalignment. The novel architecture consists of an

inductively-coupled extender (ICE) that remains in a fixed position relative to the LC sensor.

This nearly eliminates the misalignment issues between the external reader and LC-resonator.

The closed circuit design of the ICE also enables a robust signal to be realized in a lossy soil

substrate even at a depth of 1 meter. The feasibility of an ICE-LC sensor architecture is first

validated through a physical model in Matlab using an equivalent lumped-element circuit

model. Then an initial prototype is tested using soil samples with varying soil moisture

contents. The LC-resonant sensor response is then optimized via changes in ICE coil geometry.

The optimized ICE-LC sensor is then tested in cyclic soil dehydration experiments to

demonstrate correlation of resonant frequency to soil moisture content measured by

established, wired sensors and reversibility of the response. Finally, a smaller, planar form

factor of the ICE-LC is tested to demonstrate the ability to maintain diminished misalignment

sensitivity without the need for extended read range. All soil moisture content experiments

were benchmarked against a capacitive soil moisture sensor.

RESULTS

Design and Modeling of the ICE-LC Coupled Circuit

A resonant sensor system consists of an LC sensor and a wireless reader used to interrogate the

sensor to determine resonant frequency. The reader supplies an oscillating voltage to a readout

coil that inductively couples with the sensor (schematic and equivalent circuit of a typical LC

sensing system is shown in Fig. 1a,b). The impedance at the readout coil can be expressed as

$$Z_1 = j\omega L_r + \frac{\omega^2 M^2}{R_s + j\omega L_s + \frac{1}{j\omega C_s}} \tag{1}$$

where L_r, L_s, C_s, and R_s are reader coil's inductance, sensor coil's inductance, capacitance, and resistance, respectively, as shown in Figure 1a. The mutual inductance M is expressed as

$$M = k\sqrt{L_r L_s} \,, \tag{2}$$

where k is the coupling coefficient between the coupled inductors and $0 \leq k \leq 1$. According to Equation 1, the real part of the impedance will have a maximum at the resonant frequency, which is defined as

$$f_0 = \frac{1}{2\pi\sqrt{L_s C_s}} \,. \tag{3}$$

When the sensor is brought in proximity to the readout coil, the impedance begins to match, power is transferred to the LC tank, and a minimum is observed in reflected power (measured via the $|S_{11}|$ scattering parameter magnitude). Although the frequency at this minimum does not directly reflect the exact resonant frequency of the sensor due to the imaginary components of the impedance, they are still correlated and this convenient measure can be used to represent the sensor's resonant frequency. Since C_s is a function of relative permittivity of environment, the variation in soil moisture content around the sensor affects the resonant frequency. However, in practice, the resonant frequency is also dependent on the mutual position between the reader and sensor (Chan *et al.*, 2020), detailed below. Magnetic coupling requires the reader to be in close proximity with the sensor (<5 cm for typical VNA power), limiting the interrogation range of the sensor. Furthermore fertilizer and minerals present in ground water create a lossy system which further reduce the power transferred to the LC tank and thereby reduces the interrogation range of the sensor(Carr *et al.*, 2020). Adding a lossless

dielectric substrate between the resonator and the soil can help reduce the sensitivity to lossy systems with the tradeoff of decreasing the gain of the sensor.

To overcome these positional and step-off distance limitations of direct, inductive coupling between reader and hookup coil, we propose adding an additional circuit component: the ICE composed of two linked coils used for wireless power transmission (Fig. 1 c,d). This is analogous to a repeater which is used to extend read range in previous work (Kurs *et al.*, 2007; Sample, Meyer and Smith, 2011) except the coils in our application are wired together in a closed circuit (see dumbbell shape in Fig 1c) to reduce power loss to the environment. One of the coils receives power (ICE top coil) from the reader coil whereas the other interrogates (ICE bottom coil) the sensor coil like the conventional reader. In this manner, the ICE top coil is placed at the soil surface allowing for efficient inductive coupling with a reader swept at the surface and the ICE bottom coil is placed at any level below the ground to the extent that sufficient power can be transferred to the sensor. Also, because the relative positions of the buried ICE bottom coil and LC sensor are held constant, the parasitic capacitance between the coils(Demori *et al.*, 2018) are constant and the issue of positional-dependent signal can be mitigated.
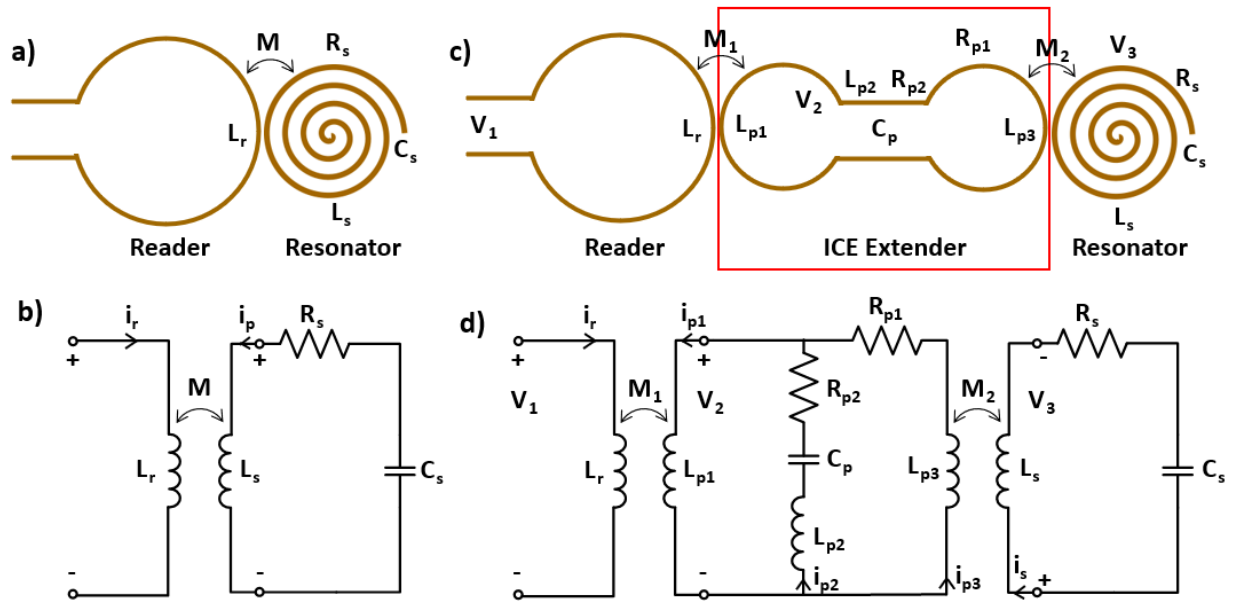
Figure 1. Schematics and equivalent circuit models of a conventional wireless resonant sensor system (a) and sensor system with inductively coupled extended reader (ICE) extender implemented (b).

To model the sensor response, Kirchhoff's voltage law is applied on the equivalent circuit (Fig.1d). Although the physical dimensions of the prototype are comparable to the wavelength of the system, causing inaccuracy when using the lumped model, the stationarity of the system still allows for approximate analysis to note for trends and provide confidence in expected sensor response. The voltages across the points defined in Fig. 1d can then be represented as

$$V_1 = j\omega L_r i_r + j\omega M_1 i_{p1} \tag{4}$$

$$
\begin{aligned}
V_2 &= j\omega L_{p1} i_{p1} + j\omega M_1 i_r \\
&= -j\omega L_{p2} i_{p2} - \frac{i_{p2}}{j\omega C_p} - R_{p2} i_{p2} \\
&= -j\omega L_{p3} i_{p3} - R_{p1} i_{p3} - j\omega M_2 i_s
\end{aligned} \tag{5}
$$

$$V_3 = j\omega L_s i_s + j\omega M_2 i_{p3} = -R_s i_s - \frac{i_s}{j\omega C_s} \tag{6}$$

where the mutual inductances are

$$M_1 = k_1\sqrt{L_r L_{p1}} \tag{7}$$

$$M_2 = k_2\sqrt{L_{p3} L_s} \tag{8}$$

The variable L_{p2} represents the inductance of the connecting wires between the two coils

whereas C_p represents the equivalent capacitance for the ICE system. The impedance at the

terminals of the readout coil is then expressed as

$$Z = \frac{V_1}{i_r} = j\omega L_r + \cfrac{\omega^2 M_1^2}{j\omega L_{p1} - \cfrac{\alpha\beta}{\alpha + \beta}} \tag{9}$$

where

$$\alpha = -j\omega L_{p2} - \frac{1}{j\omega C_p} - R_{p2}$$

$$\beta = -j\omega L_{p3} - R_{p1} + Z_s$$

$$Z_s = \cfrac{\omega^2 M_2^2}{R_s + j\omega L_s + \cfrac{1}{j\omega C_s}} \tag{10}$$

Comparing Equations 1 and 9, similarities are noted and the information from the sensor for

the modified system (Eq 10) is now used in Eq 9. The magnitude of $|S_{11}|$ resulting from

Equations 9 can then be modeled using a numerical computation package (*e.g.* Matlab). To test

the response of this system, we used parameter values that keep our resonant frequency in the

expected 50 to 200 MHz range (Supplement 1). Note that Equation 9 exhibits an additional

signal dip at ~164 MHz that corresponds to the Z_s term (the coupled sensor coil).

Using this circuit model, we can now simulate the effect of a changing soil permittivity caused by moisture content variation in Matlab. When the capacitance of the ICE (C_p) changes (modeled from 3 to 4 pF), indicative of soil permittivity at different layers of soil, the sensor resonant frequency is barely affected (less than 150 kHz shifts across the C_p span, Fig 2a). In contrast, varying the sensor capacitance term (C_s; modeled from 1 to 2 pF), indicative of change in soil moisture at the LC sensor position, results in appreciable sensor response (Fig 2b). Additional dips across the frequency range not captured by this simplified model could occur in practice (as we see in the following empirical results); these result from harmonics and other parallel resonant frequencies within the system (Supplement 2). Therefore, the sensor resonant frequency should be carefully designed such to preserve sufficient frequency range in response to the target while avoid overlapping with other dips.
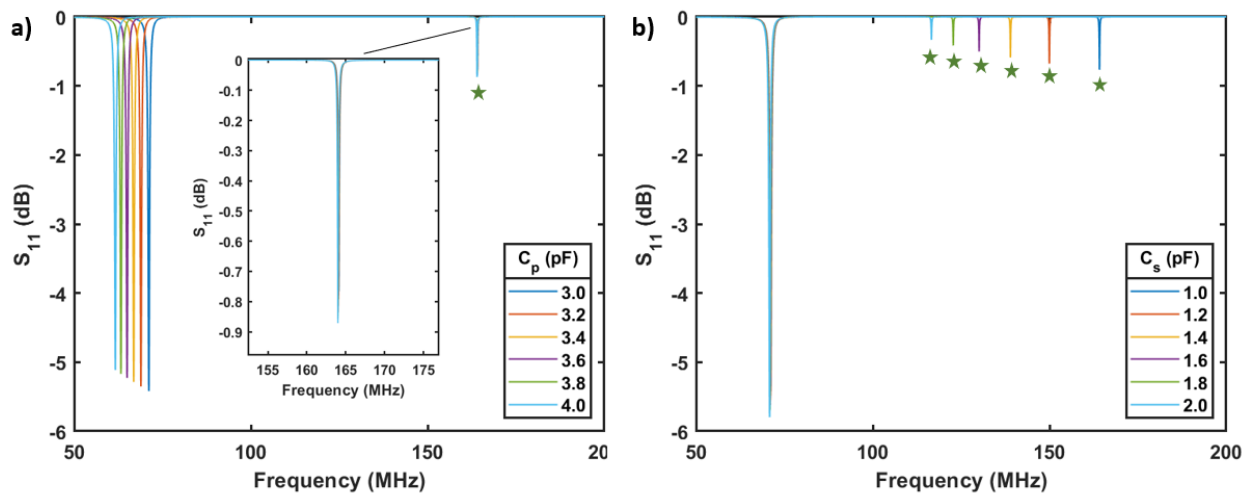

Figure 2. Simulation of frequency response of coupled ICE-LC system. (a) Effect of capacitive changes in the ICE region (not at sensor site) on the sensor response. (b) Effect of capacitive changes at the sensor

site on the resonant sensor response. Note: dips with a star indicate resonant frequencies of the LC resonator. All other peaks are from the ICE portion of ICE-LC.

Prototyping and soil moisture sensing

With confidence gained from the computational model for a clear sensor response, a prototype sensor was fabricated for optimization and simulated field testing. This was built on a wooden dowel (using the geometries shown in Table 1) for a potential read range of up to 1 meter deep in soil (Fig 3). To mitigate noise the wires connecting the two coils of the ICE system were shielded and all tests utilized the same resonant sensor affixed to the bottom coil of the ICE system. The system tested with and without the resonant sensor confirmed the interrogation between the reader and the sensor (Fig. 3a). The sensor was interrogated via the ICE-LC system at frequency dips around 140 MHz when in proximity to ICE bottom coil. These dips are dependent on the parallel LC components present within the system including that of the sensor and ICE extender. Different alignments of the reader on the top ICE coil also showed negligible effect on the resonant frequency of the sensor (Supplement 3) due to the constant parasitic capacitance between the bottom ICE coil and the sensor coil, demonstrating the system's capability to overcome positional limitations.

Next the sensor was tested in soil with varying water mass fraction, defined as the mass of water added divided by the total mass of soil and water (Fig. 3b). Note that the start resonant frequency decreased when dry soil was used compared to air as silicates and organic material in soil have a relative permittivity of around 4 compared to 1 for air. The resonant frequency and

the dip magnitude both decrease as soil moisture increases. This is consistent with higher relative permittivity of soil as more water is present, increasing the capacitance and therefore reducing the resonant frequency, as described in Equation 3. A higher moisture content also increases the conductance of the soil creating a more lossy environment and therefore decreasing the dip magnitude (less power absorbed by the LC sensor). Other parameters that cause a change in local permittivity can also affect the sensor signal. For instance, the effect of temperature was found to be 0.053 MHz decrease in resonant frequency for every degree Celsius increase (Supplement 4). Although the temperature effect on the resonant frequency is smaller than the sensor response to soil moisture for experimental ranges observed in the field, it would still be prudent for future work to mitigate confounding signal effects caused by temperature and soil structure through engineered design changes or correction factors.
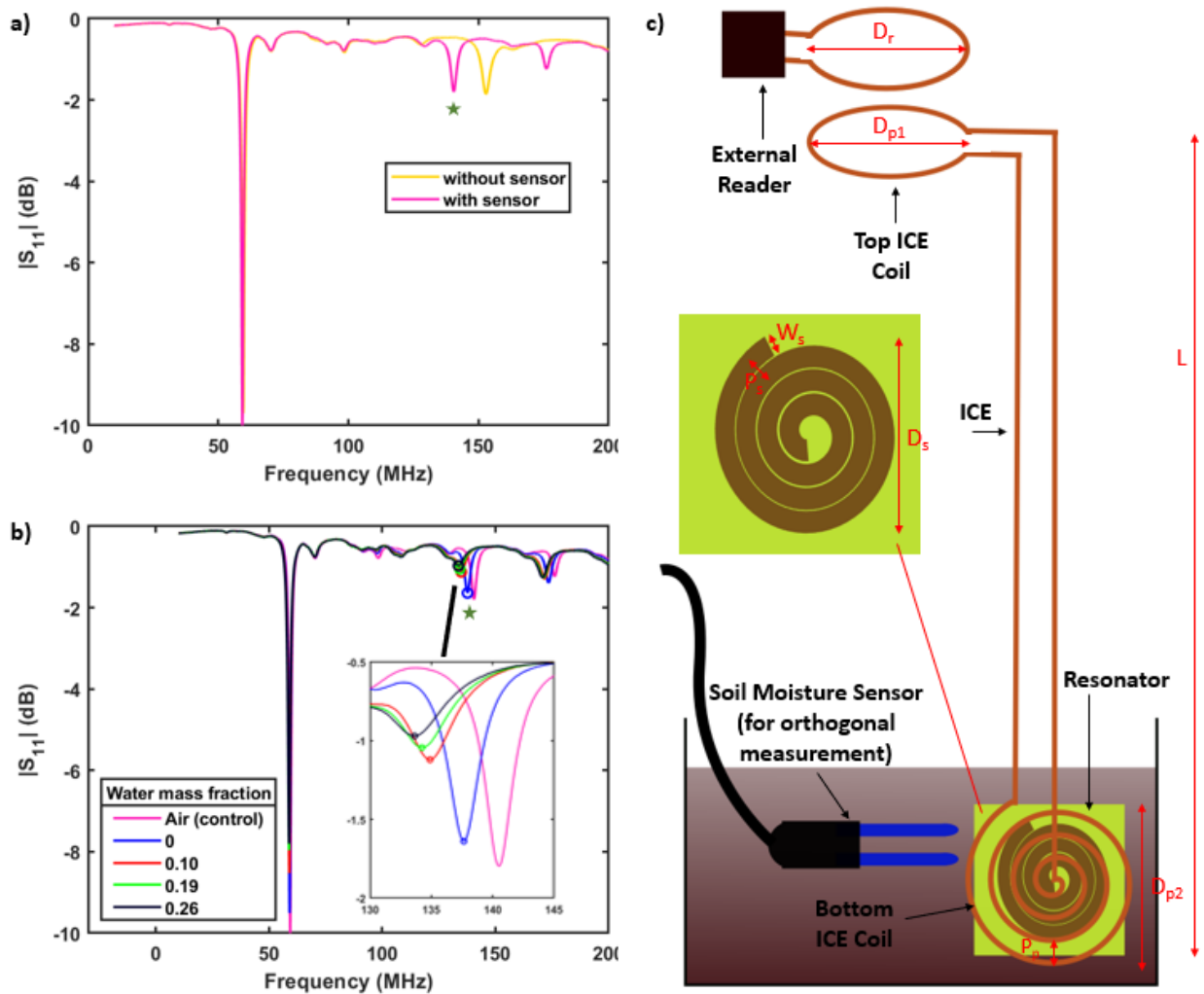
Figure 3. Testing of ICE-LC Sensor prototype with soil samples in lab. a) Effect of soil on the resonant frequency of the resonant sensor. b) Effect of increasing soil moisture content on the resonant frequency and amplitude of the resonant sensor response. c) Experimental setup including ICE-LC sensor with wireless reader and wired capacitive soil moisture sensor (for orthogonal measurement) in container of soil.

Table 1. Dimensions for prototype of ICE-LC sensor system.

System	Variable	Geometry
Reader	Outer diameter, D_r	4 cm
ICE	Top ICE coil diameter, D_{p1}	4 cm
	Bottom ICE coil diameter, D_{p2}	4 cm
	Bottom ICE coil pitch, P_p	4 mm
	Length, L	1 m
Sensor	Outer diameter, D_s	4 cm
	Pitch, P_s	2.5 mm
	Trace width, W_s	2 mm

System optimization

To further optimize the sensor response, we investigated effects of reader, ICE top, and ICE bottom coil sizes on sensor sensitivity to different soil moisture contents using four different geometries (1 turn, 4 turns (4 mm pitch), 6 turns (3 mm pitch), and 8 turns (2 mm pitch)) while keeping the outer diameters constant at 4 cm (Fig 3a). When investigating each of the coils using the above geometries, the other coils were fixed at 4 turns. These circuit geometries affect the inductances and C_p values. Varying the sizes of reader coil and ICE top coil does not affect sensor response outside of having different starting resonant frequencies of the sensor (Supplement 5). However, different geometries of ICE bottom coil yield different sensitivity, with the greatest sensitivity obtained from the single loop (Fig. 4a, b) (Supplement 5).

In terms of power transfer, the $|S_{11}|$ value at the resonant frequency of sensor is used for evaluation. Changing the geometry of reader coil resulted in most power transferred when it is at 1 turn, followed by 4 turns, 6 turns, and 8 turns (Supplement 6). On the other hand, tuning each ICE top and bottom coil both resulted in the highest power transferred with 6 turns, followed by 4, 1, and 8 turns. However, tuning the ICE top coil while having the reader and ICE bottom coils fixed at 1 and 4 turns, respectively, showed highest power transferred when the ICE top coil is 1 turn. This indicates the matching of inductance between the interrogating coils is essential for a higher power transfer. Therefore, the reader and ICE top coils are set at 1 turn each and the ICE bottom coil is set at 4 turns to provide a sufficient $|S_{11}|$ value. Using 1 turn for the ICE bottom coil results in highest sensitivity (Fig. 4b), the 4 turn geometry ensures the sensor signal is detectable in high moisture environments; the single turn ICE bottom coil did not provide detectable signal in high moisture environment with this geometry combination (data not shown).
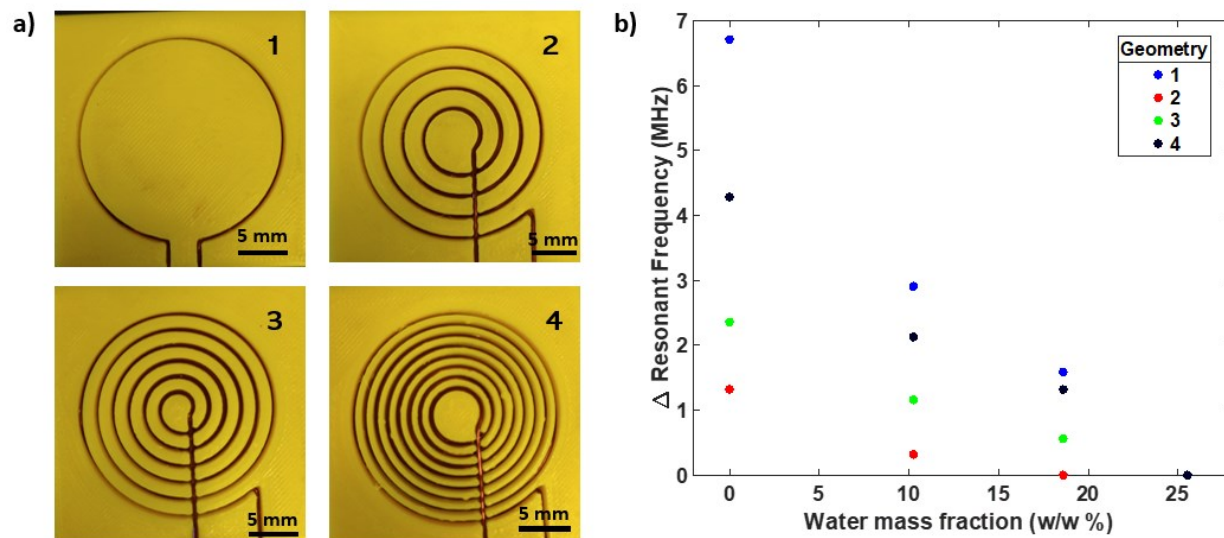
Figure 4. Different geometries of coils used for sensitivity experiments (a). Sensitivity analysis of the bottom ICE coil (b). The Δ resonant frequency is defined by the subtraction of actual resonant frequency to the minimum actual resonant frequency throughout the span of water mass fraction.

Sensor Testing with Simulated Soil Field Conditions

This optimized ICE-LC sensor was then tested with simulated field conditions of soil dehydration and rehydration events to establish metrics of sensors response (linearity, limits of detection, robustness). The ICE-LC sensor system was placed in a beaker of low clay soil hydrated to ~35% moisture content. The beaker was then continuously monitored using the ICE-LC sensor until the moisture content dried to between 20 – 25%. When tested with varied water mass fractions prior, the soil moisture content ranged between 0.8-12.5% (see Materials and Methods section). The limits of detection covered in this study range cover an even greater

range of 0.8% to 35%. Nonetheless, a higher limit of detection could still be possible with continued increase in permittivity as the soil moisture increases, however this was beyond the experimental range of our system. The dehydration process was repeated three times to determine the sensor stability and reproducibility of the sensor response to soil moisture content. Initially high clay soil was used for this experiment, but it was difficult to simulate field conditions at 1 meter depth with a smaller beaker as the high clay content soil was prone to cracking upon dehydration and rehydrating the soil resulted in mini-reservoirs, which skewed the resonance frequency response, see Supplement 7. This 'cracking' phenomenon would be a limitation to use, as the sensor relies on a homogenous soil body with smooth changes in permittivity caused by water addition, not stochastic jumps caused by cracking and flooding with water.

In general, the frequency response for the ICE-LC system correlated with a capacitive-based soil moisture sensor moisture content response (Fig. 5a). The base frequency did change after each rehydration experiment, which is likely caused by soil compaction during rehydration events, uneven water infiltration, and the difference in sensing regions of the capacitive and ICE-LC sensors, and the data was normalized to the highest resonant frequency during the rehydration event. The sensor gains (change in resonant frequency relative to change in moisture) were similar for the first and third run (insert text Fig 5b), but we observed an exceptionally lower gain in the second run. This is caused by the discontinuity observed between 30-35% moisture content that could be due to water accumulation around the LC sensor, as this initial prototype was tested without a hermetic seal. Without this outlier region, the gain for the second run

becomes 5.58, which is closer to the other cycles. A linear fit on all the independent dehydration cycles resulted in an R^2 of 0.745. Evaluating the residuals, the mean absolute error and the root mean squared error when correlating resonant frequency to soil moisture content measured by the capacitive sensor are 2.05% and 2.41%, respectively. Sources of error between methods could be electronic noise from both methods and variations in macro soil structure causing non-uniform rehydration throughout the soil (i.e., dryer on the surface where the capacitive sensor is vs. lower where the resonant sensor is placed). Ways to reduce variation in gain include standardizing fabrication of ICE-LC sensor, using polymer sleeves to protect the shielding from getting wet, and using a low loss (low relative permittivity) core material instead of a wooden dowel for the post of the sensor.
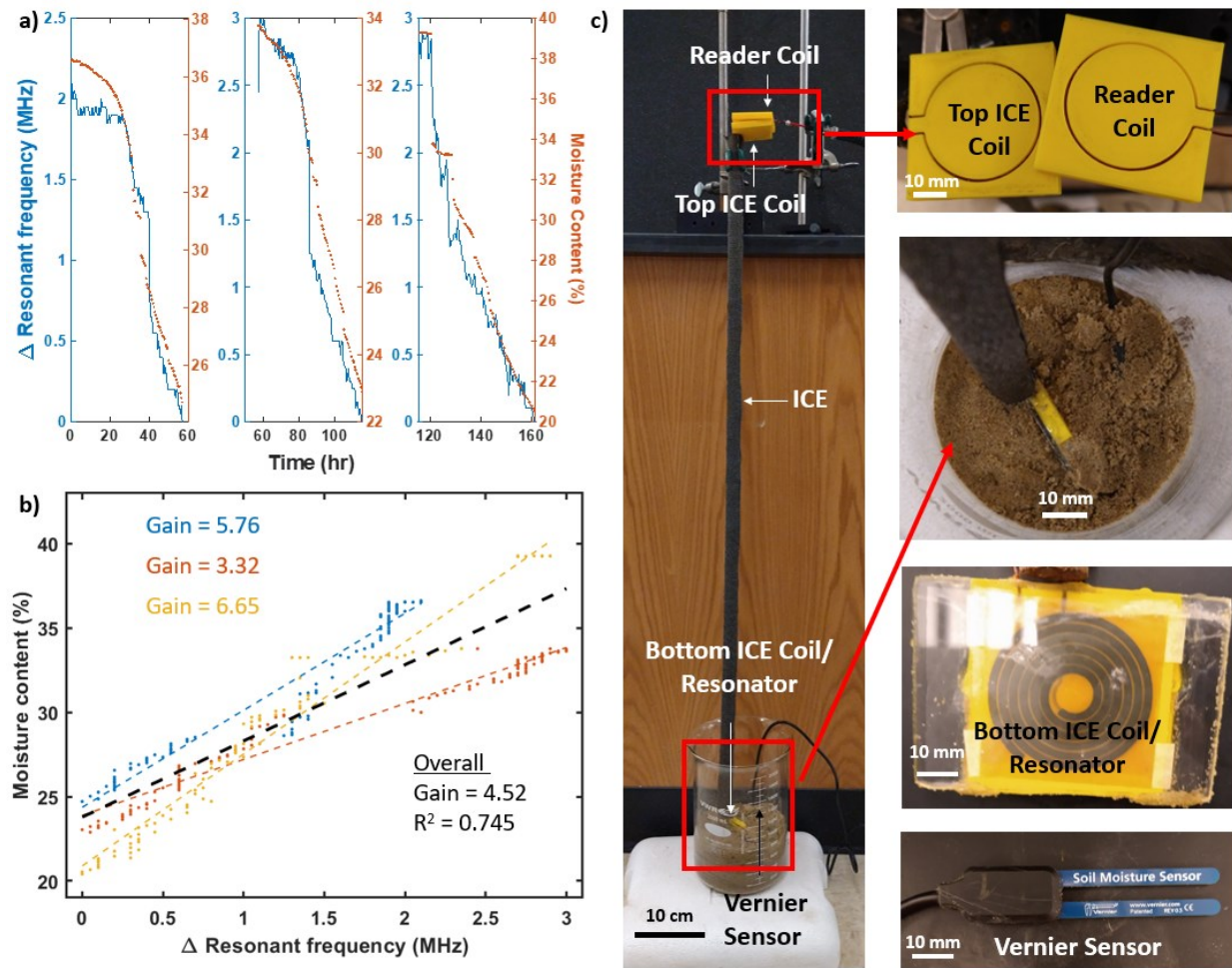
Figure 5. Simulation of field conditions with ICE-LC sensor system. a) Effect of resonant frequency as a result of decreasing soil moisture content with three dehydration periods. After the first two dehydration periods the container of soil was rehydrated. b) Parity plots and gain of the three soil dehydration experiments. c) Experimental setup of ICE-LC sensor system with external reader and a capacitive moisture sensor for orthogonal measurement.

To determine the effect of VWC along the length of the ICE-LC sensor we buried the sensor in a PVC pipe (6" diameter) with sand along with three Teros 12 soil moisture sensors buried at different depths, see Fig. 6 a,b. We monitored the frequency shift of both dips of the ICE and LC

sensor along with the VWC from the Teros 12 sensors while water flowed through the pipe. The resonant dip for the ICE resonant frequency shifted minimally as the VWC increased along the length of the ICE-LC sensor, Fig. 6 c. For the LC-sensor resonant frequency dip, the dip was insensitive to changes in VWC along the length of the ICE-LC sensor until the VWC of the soil in close proximity changed, Fig. 6 d. Insensitivity to changes in VWC along the length of the ICE and sensitivity only in close proximity of the LC sensor can be attributed to the shielding around the ICE portion of the sensor isolating the EM field away from the soil at these depths. This buried sensor experiment demonstrates the sensor's potential to be deployed at different depths and have an LC resonant frequency shift that will change only in response to changes in VWC at the depth of the LC sensor itself.
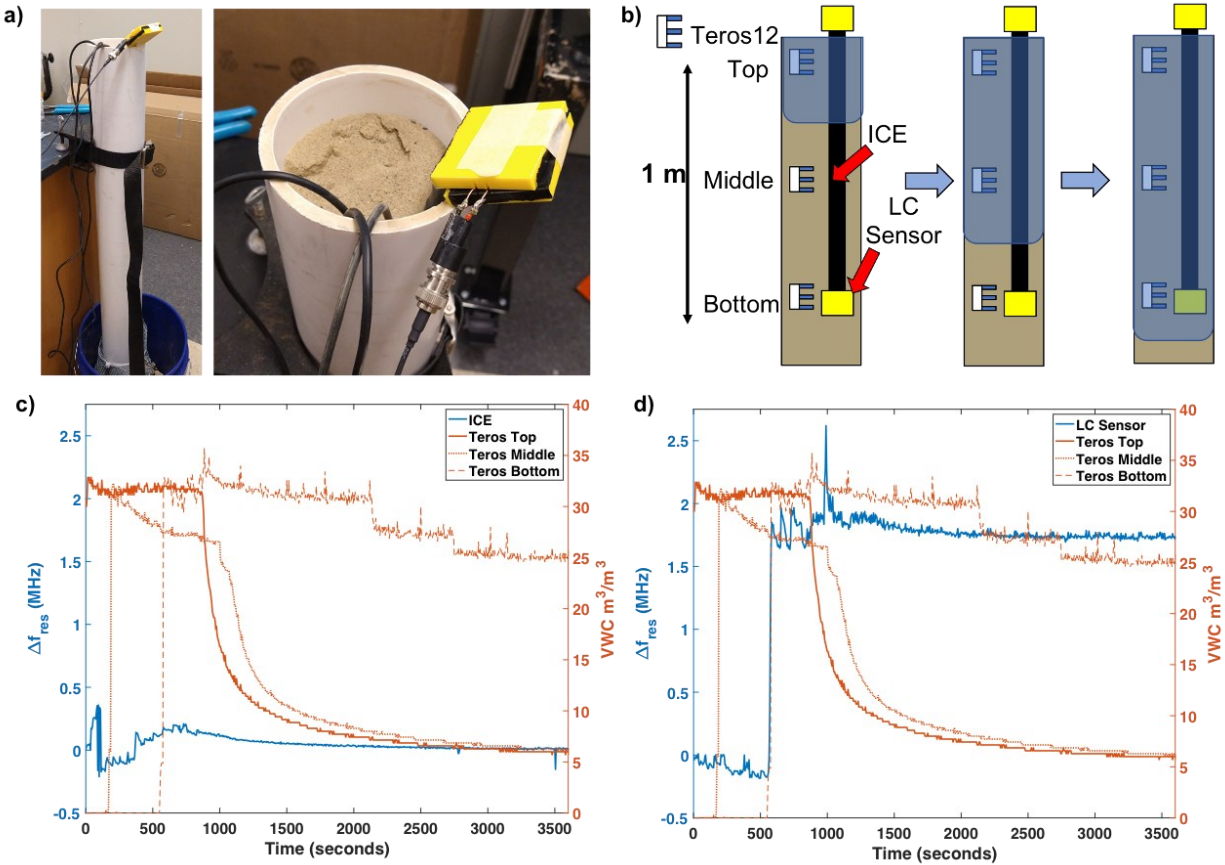
Figure 6. Photos of buried sensor experimental setup. b) Schematic of buried ICE-LC sensor experiment with three Teros12 soil moisture sensors buried at three levels up to 1 m depth. c) Resonant frequency shift of ICE frequency with changes of VWC at different depths. d) Resonant frequency shift of LC sensor frequency with changes of VWC at different depths.

Planar Compact Form Factor of ICE-LC Sensor

Finally, the ICE-LC sensor was designed in planar form to demonstrate the ability to adapt the ICE concept to different applications in soil moisture measurement and beyond. A planar version of the ICE-LC sensor was fabricated on a single sheet of copper-clad polyimide (DuPont Pyralux), attached to a glass beaker, which represents a free-standing pot or planar rhizotron, and soil moisture content was monitored through the container (Fig. 7a). The beaker was filled with soil at different water mass fractions with the soil at each water mass fraction being replaced and measured three times (Fig. 7b). To simulate a real-world scenario where an

operator would periodically assess each sensor with a handheld reader, in this experiment the reader was removed and replaced between trials (not static setup); the average standard deviations of 1.41MHz between three replicates (error bars Fig 6b) demonstrate the positional independence of the reader. A major source of this deviation is likely due to the soil structural variation between the replicates. Nonetheless, this shows that in other use scenarios where an extended read range (>5 cm) is not needed, the ICE in a compact, planar form can still be used to provide positional independence between the reader coil and LC sensor. This will have immediate impact in other LC sensor applications (temperature(Tan *et al.*, 2017), pressure(Chen, Chan and Lam, 2013; Tan *et al.*, 2017; Lin and Ma, 2018), humidity(Ong *et al.*, 2001; Deng *et al.*, 2018), strain(Butler *et al.*, 2002), chemicals(Potyrailo *et al.*, 2012), gases(Potyrailo, 2016), etc.) that suffer from positional variance.
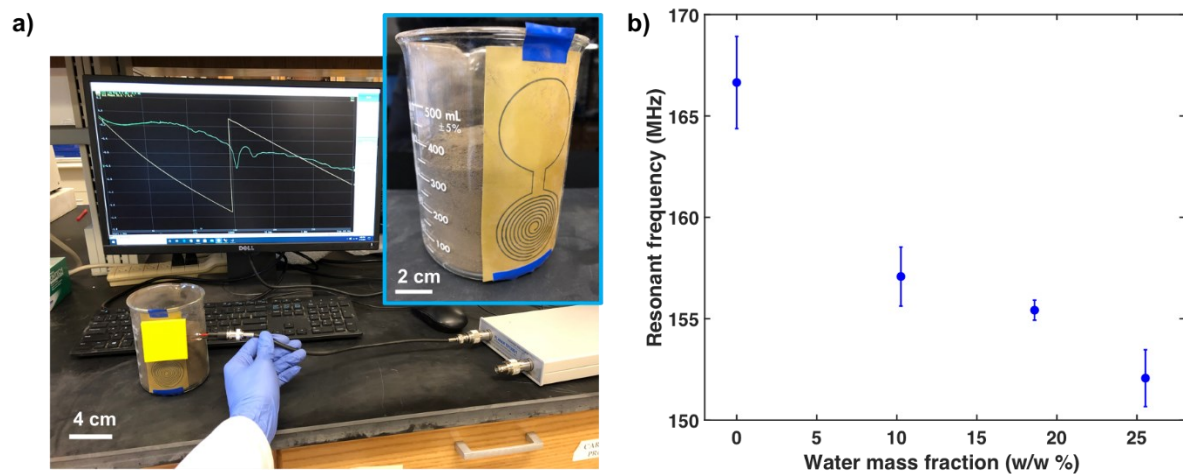

Figure 7. Planar, compact form factor for ICE-LC sensor system. a) Experimental setup of planar compact system testing soil moisture content through a glass beaker. b) Frequency response of increasing soil moisture content, n = 3.

CONCLUSION

Prior to this work, low-cost, passive LC sensors were best suited to static applications that allowed for proximal placement of the reader. This work dramatically extends possible applications of LC sensors by overcoming these step-off distance and positional limitations using an ICE-LC design. The sensor was designed and simulated using an equivalent lumped element model in MATLAB and in Advanced Design System, which showed the potential for extending read range and providing positional independence. The initial prototype was further optimized to increase the sensitivity of the resonant sensor, determining that a single loop top coil and four loop bottom coil on the ICE provides the best suitability in terms of sensitivity and signal strength for the LC resonant sensor. This best design was then tested using simulated field conditions to determine the feasibility of the sensor to monitor soil moisture conditions over a growing season. The sensor showed strong correlation (R^2 of 0.745, MAE of 2.05%) between the ICE-LC sensor frequency response and the measured soil moisture content. The linear gain (4.52% water content/MHz) was observed in the range of 20 to 35% moisture content. The ICE-LC system was also demonstrated in a planar, compact form factor to demonstrate utility in applications which require positional independence but not extended read range. Future work will improve sensor performance by focusing on manufacturing methods and materials for the sensor which will decrease parity error to established methods, reduce sensitivity to soil type/electrical conductance of soil, and improve reproducibility of sensor gain. These sensors will then be deployed to field locations to provide better spatiotemporal data for modeling and precision agriculture efforts.

ACKNOWLEDGEMENTS

MATERIALS AND METHODS

Lumped Element Circuit Model and Simulation

The equivalent circuit model is analyzed and plotted using Matlab (code provided in supplement 1). Circuit models with additional parallel RLC elements was simulated to elucidate the additional dips observed across the frequency window in practice using Advanced Design System.

Fabrication of Sensor Coil

The sensor coil is fabricated using an etching method. In brief, the spiral trace is designed in Inkscape and plotted with sharpie on a Pyralux® sheet using Silhouette cutting/plotting machine. Upon drying, the Pyralux® sheet is transferred to the etching solution consisting of 2:1 of hydrogen peroxide (3 wt%) and hydrochloric acid (37%). Finally, acetone was used to remove the sharpie mask.

Fabrication of Prototype ICE-LC System

Molds with different designs of spiral traces were designed in Solidworks and 3D printed using Ultimaker 3. Twenty-gauge copper wires were then fit into the slots of the printed molds. Wires

in between the ICE top and bottom coil were taped onto a 3 ft (0.5 inch diameter) wooden dowel which serves as support. The ends of the wires were soldered to form a complete closed circuit.

Fabrication of Reader Coil and Signal measurement

Similarly, the copper wire was fit into the 3D printed mold. The ends of the wire were soldered to BNC-wire leads, which then connects to the VNA. Copper Mountain Technologies TR1300 VNA were used for s-parameters measurement using its designed software.

Sensitivity Optimization of ICE-LC System

Reader, ICE top, and ICE bottom coils were each varied using four different geometries: 1 turn, 4 turns (4 mm pitch), 6 turns (3 mm pitch), and 8 turns (2 mm pitch), with the outer diameter being constant at 4 cm. High clay content soil were dried overnight at 120°C and crushed to smaller than 1 cm clumps. The dried soil was then measured at 350 g and added with 0, 40, 80, and 120 mL of water. The soil was then homogenized using a spatula to minimize the heterogeneity of soil, resulting in water mass fraction of 0, 0.10, 0.19, and 0.26 or soil moisture content of 0.8, 5.9, 9.6, and 12.5% (measured using capacitive sensor), respectively. Water mass fraction is defined as the mass of water divided by the combined mass of water and soil in the sample. The ICE bottom coil and the sensor were buried in the soil and the soil is swapped with the different moisture contents. The extracted resonant frequencies were normalized by subtracting with the minimum resonant frequency (at highest soil moisture content).

Soil Dehydration Experiment

Ability to monitor soil moisture content via resonant frequency of ICE-LC sensor was performed using low clay soil (play sand) samples in laboratory. A container of 600 mL of dry soil had 150 mL of water which was allowed to infiltrate freely into the soil. Soil used in experiment was air dried in oven at 60 °C overnight. The ICE-LC sensor's bottom coil and resonant sensor were buried in the soil along with a capacitive soil moisture sensor (Vernier) ~2 inches below the surface of the soil. The external reader connected to VNA was placed in proximity to the top coil of the ICE-LC sensor and automatic scans were taken every 30 minutes. At each time point the soil moisture content was also recorded according to the capacitive sensor in the soil. Soil was allowed to dehydrate until the soil moisture content was ~20-25% whereupon an additional 100 mL to rehydrate the soil. This rehydration step was repeated two times. The extracted resonant frequencies between different cycles were normalized by subtracting the maximum resonant frequency of the corresponding dehydration cycle and then adding a negative sign to match the moisture content trend measured by the capacitive sensor.

Buried Sensor Experiment

The effect of varying VWC along the length of the ICE-LC sensor was tested by burying the sensor in a PVC pipe (1.2 m in height, 10 cm in diameter) with sand. The bottom of the PVC pipe was filled with gravel and holes were drilled to allow for drainage into a 5 gallon bucket. The ICE-LC was also buried with three Teros 12 soil moisture sensors (METER) 5 cm below the top of the sand, 0.5 m below the top of the sand, and at 1 m below the top of the sand at the level of the LC resonator. The Teros 12 sensors were wired to a C1000 data logger (Campbell Scientific)

and data was collected every 5 seconds from all three sensors using SDI12 communication protocol. The resonant frequency of the ICE and LC portions of the sensor were collected using external reader connected to VNA every 5 seconds as described previously.

Soil Temperature-varying Experiment

The effect of temperature on the resonant frequency was performed in a cooling process. Water was added into a beaker containing 600g of low clay soil to soil moisture contents of 4%, 8%, and 12% (measured by Vernier). The beaker is then covered with aluminum foil and placed in an oven at 70°C for 15-20 minutes. The ICE-LC sensor's bottom coil and resonant sensor were buried in the heated soil. Amprobe TMD-56 thermocouple was used to record the temperature and was also buried and placed next to the sensor. To reduce the effect from water evaporation, the heated beaker was placed into an ice water bath to accelerate the temperature change. The VNA measurements and temperature were recorded every 30 seconds.

Fabrication and Testing of Compact Planar ICE-Sensor form factor

Similar to the sensor fabrication process above, the planar ICE-sensor was designed in Rhinoceros software and printed onto a Pyralux® and etched. The planar ICE-sensor was then taped onto the external surface of a 600 mL beaker. The beaker was filled with soil of different moisture content (same as above) and the reader coil was positioned manually and inconsistently each time when taking measurement to validate the system robustness.

REFERENCES

Babaeian, E. *et al.* (2019) 'A New Optical Remote Sensing Technique for High-Resolution Mapping of Soil Moisture', *Frontiers in Big Data*, 2(November), pp. 1–6. doi: 10.3389/fdata.2019.00037.

Babu, A. and George, B. (2018) 'An Efficient Readout Scheme for Simultaneous Measurement from Multiple Wireless Passive lC Sensors', *IEEE Transactions on Instrumentation and Measurement*. Institute of Electrical and Electronics Engineers Inc., 67(5), pp. 1161–1168. doi: 10.1109/TIM.2017.2770858.

Butler, J. C. *et al.* (2002) 'Wireless, passive, resonant-circuit, inductively coupled, inductive strain sensor', *Sensors and Actuators, A: Physical*, 102(1–2), pp. 61–66. doi: 10.1016/S0924-4247(02)00342-4.

Calvet, J. C. *et al.* (2011) 'Sensitivity of passive microwave observations to soil moisture and vegetation water content: L-band to W-band', *IEEE Transactions on Geoscience and Remote Sensing*, 49(4), pp. 1190–1199. doi: 10.1109/TGRS.2010.2050488.

Carr, A. R. *et al.* (2020) 'Sweat monitoring beneath garments using passive, wireless resonant sensors interfaced with laser-ablated microfluidics', *npj Digital Medicine*. Nature Research, 3(1). doi: 10.1038/s41746-020-0270-2.

Cassel, D. K. and Nielsen, D. R. (1986) *36 Field Capacity and Available Water Capacity*.

Chan, Y. J. *et al.* (2020) 'Wireless position sensing and normalization of embedded resonant sensors using a resonator array', *Sensors and Actuators, A: Physical*. Elsevier B.V., 303, p.

111853. doi: 10.1016/j.sna.2020.111853.

Charkhabi, S. *et al.* (2020) 'Effects of fabrication materials and methods on flexible resonant sensor signal quality', *Extreme Mechanics Letters*. Elsevier Ltd, 41, p. 101027. doi: 10.1016/j.eml.2020.101027.

Chen, G. Z., Chan, I. S. and Lam, D. C. C. (2013) 'Capacitive contact lens sensor for continuous non-invasive intraocular pressure monitoring', *Sensors and Actuators, A: Physical*. Elsevier B.V., 203, pp. 112–118. doi: 10.1016/j.sna.2013.08.029.

Crow, W. T., Kustas, W. P. and Prueger, J. H. (2008) 'Monitoring root-zone soil moisture through the assimilation of a thermal remote sensing-based soil moisture proxy into a water balance model', *Remote Sensing of Environment*, 112(4), pp. 1268–1281. doi: 10.1016/j.rse.2006.11.033.

Das, B. and Sivakugan, N. (2015) *Fundamentals of Geotechnical Engineering*.

Demori, M. *et al.* (2018) 'Electronic technique and circuit topology for accurate distance-independent contactless readout of passive LC sensors', *AEU - International Journal of Electronics and Communications*. Elsevier, 92(May), pp. 82–85. doi: 10.1016/j.aeue.2018.05.019.

Deng, W.-J. *et al.* (2018) 'Experimental Study of the Bending Effect on LC Wireless Humidity Sensors Fabricated on Flexible PET Substrates', *JMEMS Letters*, 27(5), pp. 761–763.

Dirmeyer, P. A. *et al.* (2016) 'Confronting weather and climate models with observational data from soil moisture networks over the United States', *Journal of Hydrometeorology*. American

Meteorological Society, 17(4), pp. 1049–1067. doi: 10.1175/JHM-D-15-0196.1.

Dong, L. *et al.* (2016) 'A Cyclic Scanning Repeater for Enhancing the Remote Distance of LC Passive Wireless Sensors', *IEEE Transactions on Circuits and Systems I: Regular Papers*. Institute of Electrical and Electronics Engineers Inc., 63(9), pp. 1426–1433. doi: 10.1109/TCSI.2016.2572221.

Dorigo, W. A. *et al.* (2011) 'The International Soil Moisture Network: A data hosting facility for global in situ soil moisture measurements', *Hydrology and Earth System Sciences*, 15(5), pp. 1675–1698. doi: 10.5194/hess-15-1675-2011.

Franceschelli, L. *et al.* (2020) 'A non-invasive soil moisture sensing system electronic architecture: A real environment assessment', *Sensors (Switzerland)*, 20(21), pp. 1–18. doi: 10.3390/s20216147.

Franz, T. E. *et al.* (2016) 'Using cosmic-ray neutron probes to monitor landscape scale soil water content in mixed land use agricultural systems', *Applied and Environmental Soil Science*, 2016. doi: 10.1155/2016/4323742.

Goswami, M. P., Montazer, B. and Sarma, U. (2019) 'Design and Characterization of a Fringing Field Capacitive Soil Moisture Sensor', *IEEE Transactions on Instrumentation and Measurement*. Institute of Electrical and Electronics Engineers Inc., 68(3), pp. 913–922. doi: 10.1109/TIM.2018.2855538.

Huang, Q. A., Dong, L. and Wang, L. F. (2016) 'LC Passive Wireless Sensors Toward a Wireless Sensing Platform: Status, Prospects, and Challenges', *Journal of Microelectromechanical*

Systems. doi: 10.1109/JMEMS.2016.2602298.

Kurs, A. *et al.* (2007) 'Wireless power transfer via strongly coupled magnetic resonances', *Science*, 317(5834), pp. 83–86. doi: 10.1126/science.1143254.

Lin, L. and Ma, M. (2018) 'Fabrications and Performance of Wireless LC Pressure Sensors through LTCC Technology', pp. 1–11. doi: 10.3390/s18020340.

Martini, E. *et al.* (2017) 'Repeated electromagnetic induction measurements for mapping soil moisture at the field scale: Validation with data from a wireless soil moisture monitoring network', *Hydrology and Earth System Sciences*, 21(1), pp. 495–513. doi: 10.5194/hess-21-495-2017.

Mohammadi, S. *et al.* (2020) 'Gold Coplanar Waveguide Resonator Integrated with a Microfluidic Channel for Aqueous Dielectric Detection', *IEEE Sensors Journal*. Institute of Electrical and Electronics Engineers Inc., 20(17), pp. 9825–9833. doi: 10.1109/JSEN.2020.2991349.

Mohanty, B. P. *et al.* (2017) 'Soil Moisture Remote Sensing: State-of-the-Science', *Vadose Zone Journal*. Wiley, 16(1), p. vzj2016.10.0105. doi: 10.2136/vzj2016.10.0105.

Nagahage, E. A. A. D., Nagahage, I. S. P. and Fujino, T. (2019) 'Calibration and validation of a low-cost capacitive moisture sensor to integrate the automated soil moisture monitoring system', *Agriculture (Switzerland)*. MDPI AG, 9(7). doi: 10.3390/agriculture9070141.

Nopper, R., Has, R. and Reindl, L. (2011) 'A wireless sensor readout system-circuit concept, simulation, and accuracy', in *IEEE Transactions on Instrumentation and Measurement*, pp.

2976–2983. doi: 10.1109/TIM.2011.2122110.

Nopper, R., Niekrawietz, R. and Reindl, L. (2010) 'Wireless readout of passive LC sensors', *IEEE Transactions on Instrumentation and Measurement*. doi: 10.1109/TIM.2009.2032966.

Ong, K. G. *et al.* (2001) 'Design and application of a wireless, passive, resonant-circuit environmental monitoring sensor', *Sensors and Actuators, A: Physical*. doi: 10.1016/S0924-4247(01)00624-0.

Park, P. *et al.* (2004) 'Variable Inductance Multilayer Inductor With MOSFET Switch Control', *IEEE Electron Device Letters*, 25(3), pp. 144–146. doi: 10.1109/LED.2003.822670.

Potyrailo, R. A. *et al.* (2012) 'Battery-free Radio Frequency Identi fi cation (RFID) Sensors for Food Quality and Safety'. doi: 10.1021/jf302416y.

Potyrailo, R. A. (2016) 'Multivariable Sensors for Ubiquitous Monitoring of Gases in the Era of Internet of Things and Industrial Internet', *Chemical Reviews*, 116(19), pp. 11877–11923. doi: 10.1021/acs.chemrev.6b00187.

Quiring, S. M. *et al.* (2016) 'The north American soil moisture database development and applications', *Bulletin of the American Meteorological Society*. American Meteorological Society, 97(8), pp. 1441–1460. doi: 10.1175/BAMS-D-13-00263.1.

Saleh, M. *et al.* (2016) 'Experimental evaluation of low-cost resistive soil moisture sensors', in *2016 IEEE International Multidisciplinary Conference on Engineering Technology, IMCET 2016*. Institute of Electrical and Electronics Engineers Inc., pp. 179–184. doi: 10.1109/IMCET.2016.7777448.

Sample, A. P., Meyer, D. A. and Smith, J. R. (2011) 'Analysis, experimental results, and range adaptation of magnetically coupled resonators for wireless power transfer', *IEEE Transactions on Industrial Electronics*, 58(2), pp. 544–554. doi: 10.1109/TIE.2010.2046002.

Steelman, C. M. and Endres, A. L. (2011) 'Comparison of Petrophysical Relationships for Soil Moisture Estimation using GPR Ground Waves', *Vadose Zone Journal*, 10(1), pp. 270–285. doi: 10.2136/vzj2010.0040.

Sure, A. and Dikshit, O. (2019) 'Estimation of root zone soil moisture using passive microwave remote sensing: A case study for rice and wheat crops for three states in the Indo-Gangetic basin', *Journal of Environmental Management*. Elsevier, 234(December 2018), pp. 75–89. doi: 10.1016/j.jenvman.2018.12.109.

Tan, Q. *et al.* (2017) 'A Wireless Passive Pressure and Temperature Sensor via a Dual LC Resonant Circuit in Harsh Environments'. IEEE, 26(2), pp. 351–356.

Topp, G. C., Davis, J. L. and Annan, A. P. (1980) *Electromagnetic Determination of Soil Water Content: Measurements in Coaxial Transmission Lines*, *WATER RESOURCES RESEARCH*.

Topp, G. C., Parkin, G. W. and Ferre, T. P. A. (2006) *Methods of Analysis Second Edition Soil Sampling and*.

Xu, J. *et al.* (2014) 'Measurement of Soil Water Content with Dielectric Dispersion Frequency', *Soil Science Society of America Journal*. Wiley, 78(5), pp. 1500–1506. doi: 10.2136/sssaj2013.10.0429.

Zhang, C., Wang, L. F. and Huang, Q. A. (2014) 'Extending the remote distance of LC passive

wireless sensors via strongly coupled magnetic resonances', *Journal of Micromechanics and Microengineering*. Institute of Physics Publishing, 24(12). doi: 10.1088/0960-1317/24/12/125021.